ACS APPLIED MATERIALS & INTERFACES

Research Article

www.acsami.org

Nanofibers Fabricated Using Triaxial Electrospinning as Zero Order Drug Delivery Systems

Deng-Guang Yu,*[,†] Xiao-Yan Li,[†] Xia Wang,[†] Jun-He Yang,[†] S. W. Annie Bligh,[‡] and Gareth R. Williams*[,§]

[†]School of Materials Science & Engineering, University of Shanghai for Science and Technology, 516 Jungong Road, Yangpu District, Shanghai 200093, China

[‡]Faculty of Science and Technology, University of Westminster, 115 New Cavendish Street, London W1W 6UW, U.K.

[§]UCL School of Pharmacy, University College London, 29-39 Brunswick Square, London WC1N 1AX, U.K.

Supporting Information

ABSTRACT: A new strategy for creating functional trilayer nanofibers through triaxial electrospinning is demonstrated. Ethyl cellulose (EC) was used as the filament-forming matrix in the outer, middle, and inner working solutions and was combined with varied contents of the model active ingredient ketoprofen (KET) in the three fluids. Triaxial electrospinning was successfully carried out to generate medicated nanofibers. The resultant nanofibers had diameters of 0.74 ± 0.06 μm, linear morphologies, smooth surfaces, and clear trilayer nanostructures. The KET concentration in each layer gradually increased from the outer to the inner layer. *In vitro* dissolution tests demonstrated that the nanofibers could provide linear release of KET over 20 h. The protocol reported in this study thus provides a facile approach to creating functional nanofibers with sophisticated structural features.

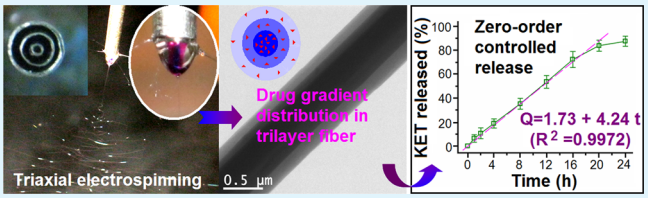

KEYWORDS: *triaxial electrospinning, trilayer structure, medicated nanofibers, gradient distribution, zero-order controlled release*

INTRODUCTION

The traditional practice of repeated oral administration of high doses of a drug at frequent time points is highly undesirable because of the risk of adverse side effects and also because of potential issues with patient compliance. As a result, controlled and sustained release drug delivery systems (DDSs) have attracted enormous amounts of research effort.[1−3] The primary method used to achieve sustained-release profiles involves the combination of active ingredients with polymeric excipients.[1,4]

In terms of the administration route, oral delivery is most widely explored because it facilitates high levels of patient compliance. However, a frequent concern associated with oral sustained-release DDS is their predisposition to an initial "burst" of drug release; this is particularly common and problematic in nanoscale DDS.[1] One nanoscale system which has attracted much attention comprises electrospun nanofibers, which are fabricated by using electrical energy to evaporate the solvent rapidly from a mixed solution containing an active ingredient and a filament-forming polymer.[5−7] The large surface area, high porosity, and commonly amorphous physical form of drugs loaded in such fibers make them very promising for the development of fast disintegrating DDS and effective delivery of poorly water-soluble drugs, whose formulation development remains one of the most intractable challenges in pharmaceutics.[6] The formation of a solid solution or suspension means that there is no lattice energy barrier to dissolution (cf. a typical crystalline active ingredient), thereby increasing both the dissolution rate and solubility in favorable instances. Unfortunately, these characteristics endow the fibers with poor performance in terms of sustained-release, owing to their usually exhibiting an uncontrollable and undesirable initial burst of release.[7,8]

To overcome this issue, coaxial electrospinning and modified coaxial electrospinning have been investigated to prepare core−sheath nanofibers with a blank (drug-free) sheath to eliminate this initial burst release.[5,7,9] Moving forward, a much sought-after class of DDS offers linear or zero-order release, because such systems can maintain the drug concentrations in a specified therapeutic window for a prolonged period of time after administration.[10] This results in high levels of patient compliance and minimal side effects.

Over the past two decades, great advances in multiple-fluid electrospinning have been achieved; this technique can create polymeric nanofibers, generate nanofiber-based composites, and produce nanofiber-based hybrids embedded with functional micro- or nanoparticles and even cells[11−15] (Figure 1). Large-scale production of electrospun nanofibers from a single-fluid has been proved to be eminently possible, and industrial systems allowing this now exist.[16−18] However, the creation of complicated nanostructures from templates at the macroscale in

Received: July 5, 2015
Accepted: August 5, 2015
Published: August 5, 2015

DOI: 10.1021/acsami.5b06007
ACS Appl. Mater. Interfaces 2015, 7, 18891−18897

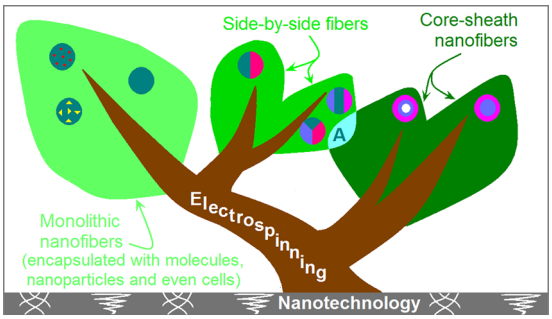

Figure 1. Development of the electrospinning process. "A" represents complicated nanostructures with side-by-side and core−sheath structures.

a "top-down" manner (i.e., using the structural characteristics of the spinneret to produce nanostructures with analogous features) has yet to be fully explored.[19] The creation of core−sheath nanostructures using a concentric spinneret has been widely reported, but there is a deficit of knowledge regarding other more complex structure types.[20−23] There are very few investigations into side-by-side electrospinning to generate Janus nanofibers[24−29] and even fewer reports on multiple-layer nanofibers.[30−35]

The slow development of multiple-fluid electrospinning processes is related to their difficulty of implementation. The successful preparation of multicomponent fibers requires the spinning fluids to have good compatibility, so that they can be drawn together by electrical forces without any coagulation. It is also necessary that the fluids have similar physicochemical properties, such that they experience similar electrical drawing forces. If one of the fluids dries faster than the others, undesirable phenomena such as the separation of fluids may occur. The more similar the working fluids are, the more successful multiple-fluid electrospinning tends to be.

Medicated nanofibers for biomedical applications are typically prepared by the addition of functional ingredients to the spinning solution. The functional moieties frequently have little influence on the electrospinnability of the working fluids. Triaxial electrospinning can thus be performed to create trilayer nanofibers in which each layer is based on the same polymer matrix but with different functional components or compositions. Using this concept, a triaxial electrospinning process in which all three working fluids contained the same polymer (ethyl cellulose, EC), but different drug contents, was developed. This permitted us to create a new type of medicated nanofibers with gradient distributions of the active ingredient. The resultant nanofibers were characterized and their drug release profiles quantified.

EXPERIMENTAL SECTION

Materials. Ethyl cellulose (EC, 6−9 mPa s) was obtained from the Shandong Ruitai Chemical Corporation (Feicheng, China). KET was purchased from the Shanghai Wanjiang Biological Technology Co., Ltd. (Shanghai, China). Anhydrous ethanol, methylene blue, and basic fuchsin were purchased from the Shanghai Chemical Reagent Company (Shanghai, China). All other chemicals used were of analytical grade, and water was doubly distilled before use.

Electrospinning. The trilayer concentric spinneret was homemade. Three syringe pumps (KDS100, Cole-Parmer, Vernon Hills, IL) and a high-voltage power supply (ZGF 60 kV/2 mA, Shanghai Sute Corp., Shanghai, China) were used for electrospinning. The collector comprised a flat piece of cardboard wrapped with aluminum foil. All electrospinning processes were carried out under ambient conditions (21 ± 5 °C with a relative humidity of 49% ± 7%). The electrospinning process was recorded using a digital camera (PowerShot A490, Canon, Tokyo, Japan). After optimization, the applied voltage and spinneret-to-collector distance were fixed at 12 kV and 15 cm, respectively. To facilitate observation of the electrospinning processes, 1×10^{-5} mg/mL of methylene blue was added to the inner fluid and 5×10^{-6} mg/mL basic fuchsin to the middle fluid.

Morphology. The morphology of the fibers was investigated using a Quanta FEG450 field emission scanning electron microscope (FESEM; FEI Corporation, Hillsboro, OR). Prior to examination, samples were sputter-coated with gold under a nitrogen atmosphere to render them electrically conductive. Images were recorded at an excitation voltage of 20 kV. The average fiber size was determined by measuring the diameters of the fibers at over 100 points in FESEM images, using the NIH ImageJ software (National Institutes of Health, Bethesda, MD). To view their cross sections, fibers were placed in liquid nitrogen and manually broken before gold coating.

Transmission electron microscope (TEM) images of the samples were recorded on a JEM 2100F field emission Instrument (JEOL, Tokyo, Japan). Samples were obtained by fixing a lacey carbon-coated copper grid on the collector and electrospinning directly onto the grid for several minutes.

Physical Form and Compatibility. X-ray diffraction was conducted over the 2θ range from 5° to 60° using a D/Max-BR diffractometer (Rigaku, Tokyo, Japan) with Cu Kα radiation at 40 kV and 30 mA. Differential scanning calorimetry was conducted using an MDSC 2910 differential scanning calorimeter (TA Instruments Co., New Castle, DE). Samples were heated at a rate of 10 °C/min from 20 to 250 °C under a 40 mL/min flow of nitrogen. Attenuated total reflectance-Fourier transform infrared (ATR-FTIR) spectroscopy was carried out on a Nicolet-Nexus 670 FTIR spectrometer (Nicolet Instrument Corporation, Madison) over the range of 500−4000 cm^{-1} at a resolution of 2 cm^{-1}.

Drug Content and in Vitro Dissolution Tests. The total drug content was determined according to the following procedure: exactly 0.1 g of the fibers was placed into 10 mL of ethanol to free the loaded KET. After complete dissolution, 1.0 mL of the ethanol solution was dropped into 100 mL of physiological saline (PS, 0.9 wt %) under agitation. Aliquots of the aqueous solutions were filtered using a 0.22 μm membrane (Millipore, Billerica, MA) before quantification using a UV−visible spectrophotometer (UV-2102PL, Unico Instrument Co. Ltd., Shanghai, China).

In vitro dissolution tests were carried out according to the Chinese Pharmacopoeia (2010 Edn.). Method II, which is a paddle method, was undertaken using a RCZ-8A dissolution apparatus (Tianjin University Radio Factory, Tianjin, China). In total, 0.2 g of the sample was placed in 600 mL of PS (37 ± 1 °C). The instrument was set to stir at 50 rpm, and sink conditions with $C < 0.2C_s$ were maintained. At predetermined time points, 5.0 mL aliquots were withdrawn from the dissolution medium and replaced with fresh medium to maintain a constant volume. After filtration through a 0.22 μm membrane and appropriate dilution with PS, samples were analyzed at λ_{max} = 260 nm. The amount of KET released was back calculated from the data obtained against a predetermined calibration curve. Experiments were performed six times, and results are reported as mean ± SD.

RESULTS AND DISCUSSION

A diagram illustrating the triaxial electrospinning process is shown in Figure 2. As for single-fluid electrospinning, the triaxial electrospinning system is composed of four components: three syringe pumps to drive the three working fluids, a high-voltage power supply, a grounded fiber collector, and a trilayer concentric spinneret.

The key to successful triaxial electrospinning is ensuring that the inner, middle, and outer laminar fluids form a compound the Taylor cone and stay together in a concentric manner throughout the electrospinning process. The physicochemical properties of a fluid, such as surface tension, conductivity, and

DOI: 10.1021/acsami.5b06007
ACS Appl. Mater. Interfaces 2015, 7, 18891−18897

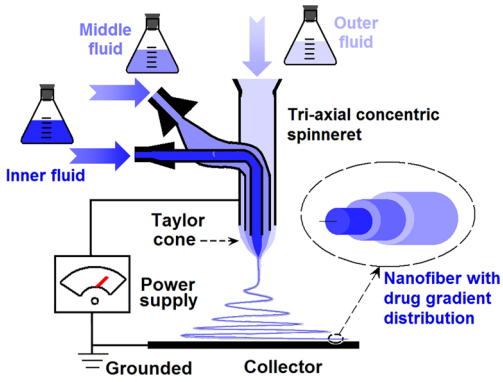

Figure 2. Schematic of the triaxial electrospinning process.

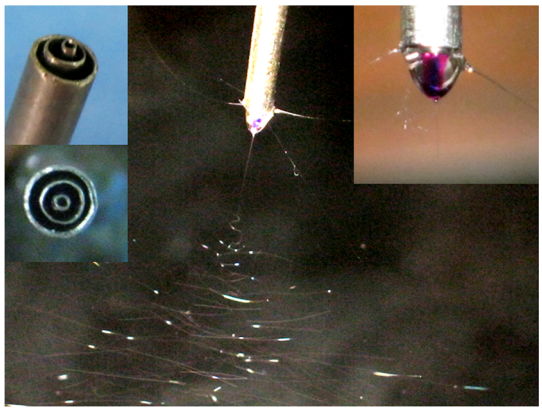

Figure 3. Digital photographs of the triaxial electrospinning process. The upper-left insets show the structure of the homemade spinneret, and the upper-right inset a typical compound Taylor cone.

viscoelasticity, determine its behavior under a high-voltage electrostatic field. Thus, in this work, very similar polymer solutions (23% w/v EC in ethanol, Table 1) with varied ketoprofen (KET) concentrations were employed as working fluids. The similarity of these solutions is anticipated to endow the three fluids with the highest compatibility and ensure similar behaviors under the electrical field.

The design of the spinneret is of critical importance in ensuring a robust and reproducible electrospinning process.[36,37] A well-designed spinneret not only provides a suitable template for producing the desired nanofiber architectures but can also allow behavioral control of the fluids under an electrical field. The trilayer spinneret used in this work is depicted in Figure 3. It consists of three concentric metal capillaries; the inner capillary has an outer diameter (D_0) of 0.4 mm and an inner diameter (D_i) of 0.20 mm, the middle capillary has D_0 of 1.1 mm and D_i of 0.9 mm, and the outer capillary has D_0 of 1.8 mm and D_i of 1.5 mm. All are made from austenitic stainless steel ($O_6Cr_{19}Ni_{10}$, GB24511, China). The end of the middle capillary projects 0.2 mm over the inner capillary, and the outer capillary similarly projects 0.2 mm over the middle capillary (upper-left inset of Figure 3). This structure is expected to promote encapsulation of the inner fluid by the middle fluid and, in turn, the middle by the outer fluid, as well as inhibiting diffusion among the fluids after ejection from the capillary nozzles.

Figure 3 shows a typical triaxial electrospinning process. A compound Taylor cone is clearly visible, from which a straight fluid jet is emitted. This is followed by an unstable region with bending and whipping loops. The three layers of the Taylor cone can be clearly discerned, as the inner and middle fluids are colored blue and pink as a result of the inclusion of methylene blue and basic fuchsin (upper-right inset of Figure 3). The connections of the spinneret to the power supply and syringe pumps are depicted in the Supporting Information. An ethanolic solution with an EC concentration of 23% (w/v) shows good electrospinnability[38,39] and, given the similarity of the three working solutions, the triaxial electrospinning process can be performed continuously and smoothly without any clogging or other adverse phenomena arising.

All three working fluids were individually electrospinnable and could be processed using single-fluid electrospinning process. Details of the resultant monolithic nanofibers are found in the Supporting Information. FESEM images of the trilayer nanofibers resulting from triaxial electrospinning and their size distributions are given in Figure 4a,b. The trilayer

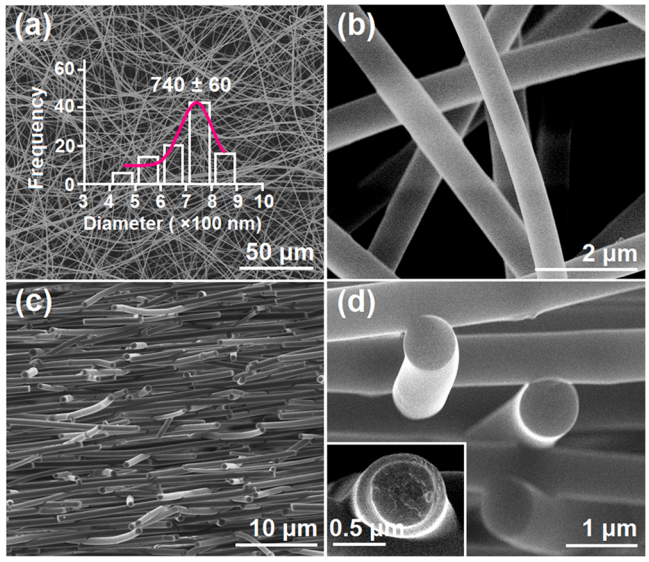

Figure 4. FESEM images of the trilayer fibers: (a) and (b) surface morphology and size distribution and (c) and (d) cross-sectional morphology. The lower left inset to part d shows an occasional instance where different layers can be observed in the cross-section.

Table 1. Preparation of Fibers with Gradient Distributions of KET in EC

	working fluid parameters[a]			solid trilayer nanofiber compositions[b]		
layer	$C_{f\text{-EC}}$ (w/v%)	$C_{f\text{-KET}}$ (w/v%)	f (mL/h)	C_{KET} (w/w%)	C_{EC} (w/w%)	
outer	23	1	2	4.17	95.83	The overall drug content in the fibers is 10.78% (w/w)
middle	23	5	0.5	17.86	82.14	
inner	23	15	0.2	39.47	60.53	

[a] $C_{f\text{-KET}}$ and $C_{f\text{-EC}}$ refer to KET and EC concentrations in the working fluids. [b] C_{KET} and C_{EC} refer to the theoretical contents of KET and EC in the different layers of the nanofibers.

DOI: 10.1021/acsami.5b06007
ACS Appl. Mater. Interfaces 2015, 7, 18891−18897

fibers have bead-free linear morphologies and smooth surfaces with an average diameter of 0.74 ± 0.06 μm. A sample of the fibers was manually broken to examine their internal cross sections (Figures 4c,d). These mainly appear smooth, although occasional irregular cross sections may also be found, as depicted in the lower left inset of Figure 4d. In such cases, the fibers may have broken such that the different layers can be discerned. Although addition of KET has little influence on the electrospinnability of the working fluids, its presence and content can influence the mechanical properties of the different layers,[40] thereby resulting in an uneven surface after breaking.

Figure 5 depicts a transmission electron microscope image of one of the fibers, which exhibits a clear trilayer structure with

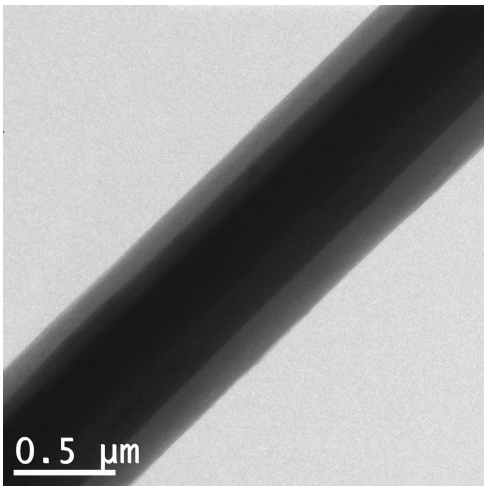

Figure 5. TEM image of a trilayer nanofiber.

the inner layer showing a very dark gray color and the outer layer showing a light gray color; these differences in color are attributed to the different drug contents of the layers. Diffusion of KET molecules from one layer to another is expected to be minimal because of the parallel flow of the three fluids and rapid drying of the layers during electrospinning.[41]

The presence of a large number of distinct reflections in the X-ray diffraction (XRD) pattern of KET (Figure 6a) confirms that the drug is a crystalline material. The diffraction pattern of EC exhibits a diffuse background pattern with two diffraction halos, which is to be expected since it is known to be amorphous. In the XRD pattern of the trilayer nanofibers, no characteristic KET reflections are visible, which demonstrates that KET is no longer present as a crystalline material in the fibers and has been converted into an amorphous state within all three layers of the polymer matrix. The differential scanning calorimetry (DSC) thermograms in Figure 6b concur with the XRD results. KET displays a distinct melting endothermic peak at 95.9 °C (ΔH_f = −115.1 J/g); in contrast, no melting events can be seen in the traces of EC and the trilayer nanofibers.

KET molecules possess carbonyl groups (potential proton receptors), whereas EC molecules have free hydroxyl groups (potential proton donors for hydrogen bonding; Figure 6c). Thus, hydrogen bonding may occur in the fibers and is confirmed by their IR spectrum. Here, the characteristic peaks of pure KET at 1697 and 1658 cm^{-1} (attributed to the vibrations of carbonyl groups) cannot be observed. Other secondary interactions, such as hydrophobic interactions between the benzene rings and the carbon chains of EC, may also play a role in the formation of EC-KET nanocomposites.

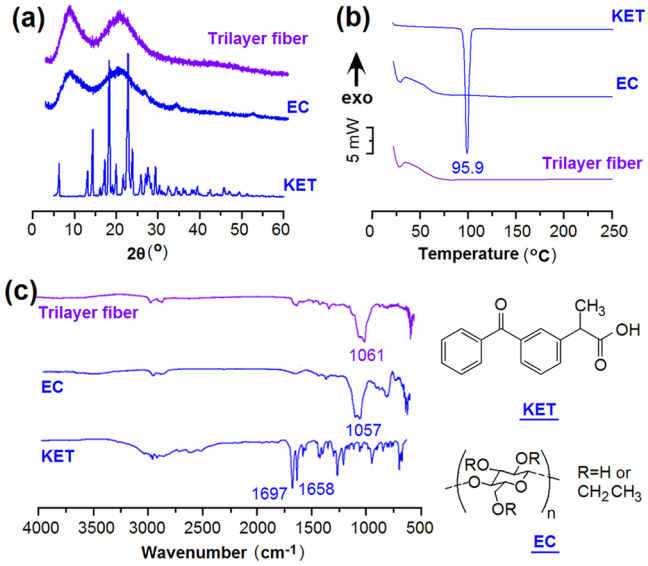

Figure 6. Characterization of the raw materials and the KET-loaded fibers: (a) XRD patterns, (b) DSC thermograms, and (c) IR spectra and chemical structures of KET and EC.

KET has λ_{max} = 260 nm, and thus a calibration curve was constructed at this wavelength: $C = 14.96A - 0.0013$ (R = 0.9999), where C is the KET concentration (μg/mL) and A is the solution absorbance at 260 nm (linear range, 2−20 μg/mL). The measured KET loading in the fibers was 108.1 ± 3.4 mg/g (n = 3), almost equivalent to the theoretically calculated value of 107.8 mg/g.

Monolithic nanofibers prepared individually from each of the three working solutions using single-fluid electrospinning have similar drug release profiles. An initial burst release is followed by a slowing in the release rate (Figure 7a, other details may be found in the Supporting Information). In sharp contrast, the three-layer nanofibers were able to provide zero-order KET release for over 20 h with a best-fit equation of $Q = 1.73 + 4.24t$ (R^2 = 0.9972), where Q is the drug release percentage, t is the release time, and R is the correlation coefficient (Figure 7b). The initial burst release and the slow-down at the end of the dissolution process are negative phenomena that inevitably arise with monolithic drug-loaded nanofibers (and also many traditional sustained-release DDS).[42,43] No burst release was observed from the triaxial nanofibers, and the drug was released at a constant rate for nearly 1 day. EC is insoluble in water, and thus the drug release is expected to arise from diffusion of the drug out of the fibers and into the dissolution milieu. FESEM images of the trilayer nanofibers after complete KET release are included in Figure 7c,d. The surfaces and cross sections of the trilayer nanofibers are wrinkled, which indicates they may have collapsed following the formation of voids when KET is freed into solution.

The surface area of the middle layer of the fibers is smaller than that of the outermost layer, and the inner layer has a still smaller surface area (Si < Sm < So; see Figure 7e). In addition, the distances through which the drug molecules must diffuse to reach the dissolution medium gradually increase going from the exterior to the interior of the fibers (Ri > Rm > Ro; Figure 7e). These factors would normally result in an initial burst release because of the large surface area at the outermost layer and the short distance through which escaping drug molecules must diffuse. However, by gradually increasing the drug concen-

DOI: 10.1021/acsami.5b06007
ACS Appl. Mater. Interfaces 2015, 7, 18891−18897

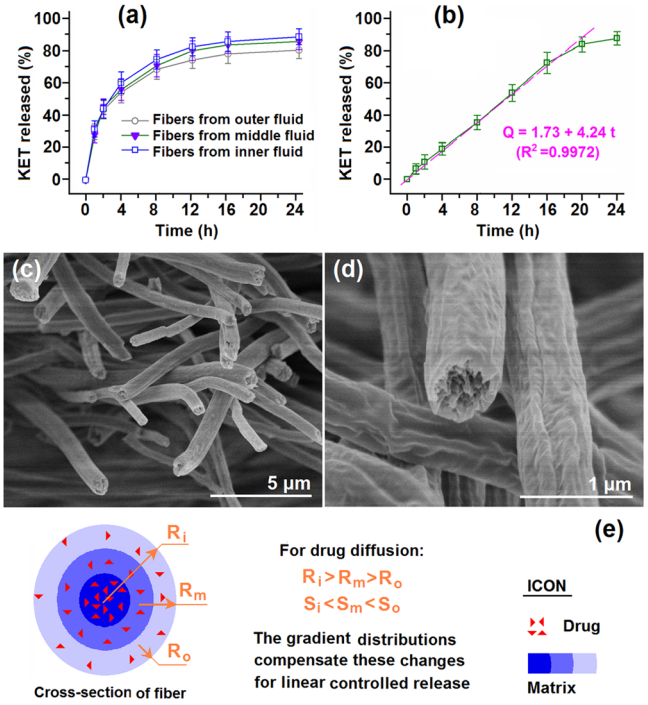

Figure 7. (a, b) In vitro dissolution test results for (a) the monolithic nanofibers and (b) the trilayer nanofibers, (c, d) FESEM images of the trilayer nanofibers after release of all the KET loading, and (e) a diagram explaining how the gradient drug distribution can yield a linear release profile.

trations in the middle and inner layers, the effects of surface area and diffusion distance on the sustained-release profile of the nanofibers can be counteracted, resulting in the desired linear release profile.

CONCLUSIONS AND PERSPECTIVES

The facile preparation of trilayer nanofibers using a triaxial electrospinning process was successfully demonstrated in this work. Triaxial electrospinning could be continuously and smoothly performed using inner, middle, and outer working fluids containing the same concentration of EC but varied concentrations of the functional ingredient KET. These fluids were highly compatible and behaved similarly under the electric field. The resultant fibers were structural nanocomposites with a linear morphology, smooth surfaces, and clear three-layer structures. The content of KET was designed to incrementally increase moving from the exterior of the fibers inward, resulting in a gradient distribution of the drug. This led to a system able to provide zero-order release for over 20 h. By incorporating this formulation into an enteric-coated capsule, a linear release colon-targeted oral drug delivery system can be produced.

This study developed an advanced functional nanomaterial using a triaxial electrospinning process and solutions of the same filament-forming polymer matrix for all three working fluids. A range of different types of functional materials and electrospinning processes can be generated from this simple procedure. Several examples include

(1) Incorporation of different ingredients in the layers of the trilayer fibers for multifunctional materials. Different functional ingredients or even inorganic nanoparticles could be encapsulated into the different layers of the fibers for a combined action, synergistic action, or to exert multiple functions. Such multifunctional fiber mats might find important applications as scaffolds in tissue engineering.[44,45]

(2) New trilayer templates for creating structural inorganic products and manipulating molecular self-assembly. Electrospun nanofibers are often indirectly used as templates for creating inorganic nanofibers, nanotubes, or carbon nanofibers. A wide variety of functional inorganic nanofibers (containing for instance metallic oxides and metals), nanotubes, and carbon nanofibers with varied compositions could be generated by loading different materials in the layers of the fibers.

(3) New triaxial electrospinning processes. New types of triaxial electrospinning processes can be further developed through careful consideration of the compatibility between working solutions. For instance, our method could be used to develop gas-assisted melt triaxial electrospinning, wherein an auxiliary gas flows through the outer capillary, similar to gas-assisted melt coaxial electrospinning.[46] Solvents, solutions of small molecules, or unspinnable dilute polymer solutions can be used as outer fluids to yield a series of modified triaxial electrospun products, similar to those which have been generated using modified coaxial electrospinning.[47−49]

(4) Implementation of other types of multiple-fluid electrospinning for creating complicated functional nanostructures. Many other types of nanoscale architectures, such as side-by-side or combinations of side-by-side and core−sheath materials, may also be obtained (Figure 1).

ASSOCIATED CONTENT

Supporting Information

The Supporting Information is available free of charge on the ACS Publications website at DOI: 10.1021/acsami.5b06007.

Experimental details and additional results (PDF)

AUTHOR INFORMATION

Corresponding Authors

*Phone: +86-21-55270632. Fax: +86-21-55270632. E-mail: ydg017@usst.edu.cn.

*Phone: +44-(0)207-7535868. E-mail: g.williams@ucl.ac.uk

Notes

The authors declare no competing financial interest.

ACKNOWLEDGMENTS

This work was supported by the Natural Science Foundation of Shanghai (Grant No. 13ZR1428900), the China NSFC/UK Royal Society Cost Share International Exchanges Scheme (Grant No. 51411130128/IE131748), the National Science Foundation of China (Grant Nos. 51373101, 51373100, and 5140030478), and the Hujiang Foundation of China (Grant No. B14006).

REFERENCES

(1) Mitragotri, S.; Burke, P. A.; Langer, R. Overcoming the Challenges in Administering Biopharmaceuticals: Formulation and Delivery Strategies. *Nat. Rev. Drug Discovery* **2014**, *13*, 655−672.

(2) Liu, W.; Thomopoulos, S.; Xia, Y. Electrospun Nanofibers for Regenerative Medicine. *Adv. Healthcare Mater.* **2012**, *1*, 10−25.

(3) Allen, T. M.; Cullis, P. R. Drug Delivery Systems: Entering the Mainstream. *Science* **2004**, *303*, 1818−1822.

(4) Hubbell, J. A.; Chikoti, A. Nanomaterials for Drug Delivery. *Science* **2012**, *337*, 303−305.

(5) Kim, Y. J.; Ebara, M.; Aoyagi, T. A Smart Hyperthermia Nanofiber with Switchable Drug Release for Inducing Cancer Apoptosis. *Adv. Funct. Mater.* **2013**, *23*, 5753−5761.

DOI: 10.1021/acsami.5b06007
ACS Appl. Mater. Interfaces 2015, 7, 18891−18897

(6) Yu, D. G.; Shen, X. X.; Brandford-White, C.; White, K.; Zhu, L. M.; Bligh, S. W. A. Oral Fast-Dissolving Drug Delivery Membranes Prepared from Electrospun Polyvinylpyrrolidone Ultrafine Fibers. *Nanotechnology* **2009**, *20*, 055104.
(7) Yu, D. G.; Li, X. Y.; Wang, X.; Chian, W.; Liao, Y. Z.; Li, Y. Zero-order Drug Release Cellulose Acetate Nanofibers Prepared Using Coaxial Electrospinning. *Cellulose* **2013**, *20*, 379−389.
(8) Taepaiboon, P.; Rungsardthong, U.; Supaphol, P. Effect of Cross-Linking on Properties and Release Characteristics of Sodium Salicylate-Loaded Electrospun Poly(vinyl alcohol) Fibre Mats. *Nanotechnology* **2007**, *18*, 175102.
(9) Wu, X. M.; Branford-White, C.; Yu, D. G.; Chatterton, N. P.; Zhu, L. M. Preparation of Core-Shell PAN Nanofibers Encapsulated α-Tocopherol Acetate and Ascorbic Acid 2-Phosphate for Photo-protection. *Colloids Surf., B* **2011**, *82*, 247−252.
(10) Xiang, A.; McHugh, A. J. Quantifying Sustained Release Kinetics from A Polymer Matrix Including Burst Effects. *J. Membr. Sci.* **2011**, *371*, 211−218.
(11) Lee, H. J.; Park, Y. H.; Koh, W. G, Fabrication of Nanofiber Microarchitectures Localized within Hydrogel Microparticles and Their Application to Protein Delivery and Cell Encapsulation. *Adv. Funct. Mater.* **2013**, *23*, 591−597.
(12) Sridhar, R.; Madhaiyan, K.; Sundarrajan, S.; Gora, A.; Venugopal, J. R.; Ramakrishna, S. Cross-Linking of Protein Scaffolds for Therapeutic Applications: PCL Nanofibers Delivering Riboflavin for Protein Cross-Linking. *J. Mater. Chem. B* **2014**, *2*, 1626−1633.
(13) Zhang, C. L.; Yu, S. H. Nanoparticles Meet Electrospinning: Recent Advanced and Future Prospects. *Chem. Soc. Rev.* **2014**, *43*, 4423−4448.
(14) Sun, B.; Long, Y. Z.; Zhang, H. D.; Li, M. M.; Duvail, J. L.; Jiang, X. Y.; Yin, H. L. Advances in Three-Dimensional Nanofibrous Macrostructures *via* Electrospinning. *Prog. Polym. Sci.* **2014**, *39*, 862−890.
(15) Sridhar, R.; Lakshminarayanan, R.; Madhaiyan, K.; Barathi, V. A.; Chin Lim, K. H.; Ramakrishna, S. Electrosprayed Nanoparticles and Electrospun Nanofibers Based on Natural Materials: Applications in Tissue Regeneration, Drug Delivery and Pharmaceuticals. *Chem. Soc. Rev.* **2015**, *44*, 790−814.
(16) Nagy, Z. K.; Balogh, A.; Démuth, B.; Pataki, H.; Vigh, T.; Szabó, B.; Molnár, K.; Schmidt, B. T.; Horák, P.; Marosi, G.; Verreck, G.; Van Assche, I.; Brewster, M. E. High Speed Electrospinning for Scaled-up Production of Amorphous Solid Dispersion of Itraconazole. *Int. J. Pharm.* **2015**, *480*, 137−142.
(17) Agarwal, S.; Greiner, A.; Wendorff, J. H. Functional Materials by Electrospinning of Polymers. *Prog. Polym. Sci.* **2013**, *38*, 963−991.
(18) Long, Y. Z.; Yu, M.; Sun, B.; Gu, C. Z.; Fan, Z. Recent Advances in Large-Scale Assembly of Semiconducting Inorganic Nanowires and Nanofibers for Electronics, Sensors and Photovoltaics. *Chem. Soc. Rev.* **2012**, *41*, 4560−4580.
(19) Chen, G.; Xu, Y.; Yu, D. G.; Zhang, D. F.; Chatterton, N. P.; White, K. N. Structure-Tunable Janus Fibers Fabricated Using Spinnerets with Varying Port Angles. *Chem. Commun.* **2015**, *51*, 4623−3626.
(20) Jiang, H.; Wang, L.; Zhu, K. Coaxial Electrospinning for Encapsulation and Controlled Release of Fragile Water-Soluble Bioactive Agents. *J. Controlled Release* **2014**, *193*, 296−303.
(21) Ji, X.; Yang, W.; Wang, T.; Mao, C.; Guo, L.; Xiao, J.; He, N. Coaxially Electrospun Core/Shell Structured Poly(L-lactide) Acid/Chitosan Nanofibers for Potential Drug Carrier in Tissue Engineering. *J. Biomed. Nanotechnol.* **2013**, *9*, 1672−1678.
(22) Wang, T.; Ji, X.; Jin, L.; Feng, Z.; Wu, J.; Zheng, J.; Wang, H.; Xu, Z. W.; Guo, L.; He, N. Fabrication and Characterization of Heparin-Grafted Poly−L−lactic acid−Chitosan Core−Shell Nanofibers Scaffold for Vascular Gasket. *ACS Appl. Mater. Interfaces* **2013**, *5*, 3757−3763.
(23) Zhang, X.; Aravindan, V.; Kumar, P. S.; Liu, H.; Sundaramurthy, J.; Ramakrishna, S.; Madhavi, S. Synthesis of TiO_2 Hollow Nanofibers by Coaxial electrospinning and Its Superior Lithium Storage Capability in Full-Cell Assembly with Olivine Phosphate. *Nanoscale* **2013**, *5*, 5973−5980.
(24) Liu, Z.; Sun, D. D.; Guo, P.; Leckie, J. O. An Efficient Bicomponent TiO_2/SnO_2 Nanofiber Photocatalyst Fabricated by Electrospinning with A Side-by-Side Dual Spinneret Method. *Nano Lett.* **2007**, *7*, 1081−1085.
(25) Chen, S.; Hou, H.; Hu, P.; Wendorff, J. H.; Greiner, A.; Agarwal, S. Effect of Different Bicomponent Electrospinning Techniques on the Formation of Polymeric Nanosprings. *Macromol. Mater. Eng.* **2009**, *294*, 781−786.
(26) Lin, T.; Wang, H.; Wang, X. Self-Crimping Bicomponent Nanofibers Electrospun from Polyacrylonitrile and Elastomeric Polyurethane. *Adv. Mater.* **2005**, *17*, 2699−2703.
(27) Srivastava, Y.; Marquez, M.; Thorsen, T. Microfluidic Electrospinning of Biphasic Nanofibers with Janus Morphology. *Biomicrofluidics* **2009**, *3*, 012801.
(28) Starr, J. D.; Andrew, J. S. Janus-Type Bi-Phasic Functional Nanofibers. *Chem. Commun.* **2013**, *49*, 4151−4153.
(29) Starr, J. D.; Budi, M. A. K.; Andrew, J. S. Processing-Property Relationships in Electrospun Janus-Type Biphasic Ceramic Nanofibers. *J. Am. Ceram. Soc.* **2015**, *98*, 12−19.
(30) Labbaf, S.; Deb, S.; Camma, G.; Stride, E.; Edirisinghe, M. Preparation of Multi-Component Drug Delivery Nanoparticles Using a Triple-Needle Electrohydrodynamic Device. *J. Colloid Interface Sci.* **2013**, *409*, 245−254.
(31) Han, D.; Steckl, A. Triaxial Electrospun Nanofiber Membranes for Controlled Dual Release of Functional Molecules. *ACS Appl. Mater. Interfaces* **2013**, *5*, 8241−8245.
(32) Jiang, S.; Duan, G.; Zussman, E.; Greiner, A.; Agarwal, S. Highly Flexible and Tough Concentric Tri-Axial Polystyrene Fibers. *ACS Appl. Mater. Interfaces* **2014**, *6*, 5918−5923.
(33) Labbaf, S.; Ghanbar, H.; Stride, E.; Edirisinghe, M. Preparation of Multilayered Polymeric Structures Using a Novel Four-Needle Coaxial Electrohydrodynamic Device. *Macromol. Rapid Commun.* **2014**, *35*, 618−623.
(34) Liu, W.; Ni, C.; Chase, D. B.; Rabolt, J. F. Preparation of Multilayer Biodegradable Nanofibers by Triaxial Electrospinning. *ACS Macro Lett.* **2013**, *2*, 466−468.
(35) Starr, J. D.; Andrew, J. S. A Route to Synthesize Multifunctional Tri-phase Nanofibers. *J. Mater. Chem. C* **2013**, *1*, 2529−2533.
(36) Zhao, Y.; Cao, X.; Jiang, L. Bio-Mimic Multichannel Microtubes by A Facile Method. *J. Am. Chem. Soc.* **2007**, *129*, 764−765.
(37) Yu, D. G.; Branford-White, C.; Bligh, S. W. A.; White, K.; Chatterton, N. P.; Zhu, L. M. Improving Polymer Nanofiber Quality Using A Modified Co-Axial Electrospinning Process. *Macromol. Rapid Commun.* **2011**, *32*, 744−750.
(38) Huang, L. Y.; Branford-White, C.; Shen, X. X.; Yu, D. G.; Zhu, L. M. Time-Engineered Biphasic Drug Release by Electrospun Nanofiber Meshes. *Int. J. Pharm.* **2012**, *436*, 88−96.
(39) Yu, D. G.; Wang, X.; Li, X. Y.; Chian, W.; Li, Y.; Liao, Y. Z. Electrospun Biphasic Drug Release Polyvinylpyrrolidone/Ethyl Cellulose Core/Sheath Nanofibers. *Acta Biomater.* **2013**, *9*, 5665−5672.
(40) Li, X. Y.; Wang, X.; Yu, D. G.; Ye, S.; Kuang, Q. K.; Yi, Q. W.; Yao, X. Z. Electrospun Borneol-PVP Nanocomposites. *J. Nanomater.* **2012**, *2012*, 1.
(41) Squires, T. M.; Quake, S. R. Microfluidics: Fluid Physics at the Nanoliter Scale. *Rev. Mod. Phys.* **2005**, *77*, 977−1026.
(42) Verreck, G.; Chun, I.; Rosenblatt, J.; Dijck, A. V.; Mensch, J.; Noppe, M.; Brewster, M. E. Incorporation of Drugs in an Amorphous State into Electrospun Nanofibers Composed of A Water-Insoluble, Nonbiodegradable Polymer. *J. Controlled Release* **2003**, *92*, 349−360.
(43) Kim, C. J. Compressed Doughnut-Shaped Tablets with Zero-Order Release Kinetics. *Pharm. Res.* **1995**, *12*, 1045−1048.
(44) Ji, X.; Wang, T.; Guo, L.; Xiao, J.; Li, Z.; Zhang, L.; Deng, Y.; He, N. Effection of Nano-ZnO on the Mechanical Property and Piocompatibility of Electrospun Poly(L-lactide) Acid/Nano-ZnO Mats. *J. Biomed. Nanotechnol.* **2013**, *9*, 417−423.

DOI: 10.1021/acsami.5b06007
ACS Appl. Mater. Interfaces 2015, 7, 18891−18897

(45) Yang, W.; Fu, J.; Wang, D.; Wang, T.; Wang, H.; Jin, S.; He, N. Study on CS/PCL Blending Vascular Scaffolds by Electrospinning. *J. Biomed. Nanotechnol.* **2010**, *6*, 254−259.
(46) Zhmayev, E.; Cho, D.; Joo, Y. L. Nanofibers from Gas-Assisted Polymer Melt Electrospinning. *Polymer* **2010**, *51*, 4140−4144.
(47) Yu, D. G.; Liao, Y.; Li, X.; Chian, W.; Li, Y.; Wang, X. Colon-Targeted Drug Delivery Core-Sheath Nanofibers Prepared Using A Modified Coaxial Electrospinning. *J. Controlled Release* **2013**, *172*, 26.
(48) Han, D.; Steckl, A. Superhydrophobic and Oleophobic Fibers by Coaxial Electrospinning. *Langmuir* **2009**, *25*, 9454−9462.
(49) Yu, D. G.; Chian, W.; Wang, X.; Li, X. Y.; Li, Y.; Liao, Y. Z. Linear Drug Release Membrane Prepared by A Modified Coaxial Electrospinning Process. *J. Membr. Sci.* **2013**, *428*, 150−156.

DOI: 10.1021/acsami.5b06007
ACS Appl. Mater. Interfaces 2015, 7, 18891−18897